Lab on a Chip

PAPER

View Article Online
View Journal | View Issue

Cite this: *Lab Chip*, 2016, **16**, 3929

Diagnosis of iron deficiency anemia using density-based fractionation of red blood cells†

Jonathan W. Hennek,[a] Ashok A. Kumar,[a] Alex B. Wiltschko,[bc] Matthew R. Patton,[a] Si Yi Ryan Lee,[a] Carlo Brugnara,[d] Ryan P. Adams[b] and George M. Whitesides*[ae]

Iron deficiency anemia (IDA) is a nutritional disorder that impacts over one billion people worldwide; it may cause permanent cognitive impairment in children, fatigue in adults, and suboptimal outcomes in pregnancy. IDA can be diagnosed by detection of red blood cells (RBCs) that are characteristically small (microcytic) and deficient in hemoglobin (hypochromic), typically by examining the results of a complete blood count performed by a hematology analyzer. These instruments are expensive, not portable, and require trained personnel; they are, therefore, unavailable in many low-resource settings. This paper describes a low-cost and rapid method to diagnose IDA using aqueous multiphase systems (AMPS)—thermodynamically stable mixtures of biocompatible polymers and salt that spontaneously form discrete layers having sharp steps in density. AMPS are preloaded into a microhematocrit tube and used with a drop of blood from a fingerstick. After only two minutes in a low-cost centrifuge, the tests (n = 152) were read by eye with a sensitivity of 84% (72–93%) and a specificity of 78% (68–86%), corresponding to an area under the curve (AUC) of 0.89. The AMPS test outperforms diagnosis by hemoglobin alone (AUC = 0.73) and is comparable to methods used in clinics like reticulocyte hemoglobin concentration (AUC = 0.91). Standard machine learning tools were used to analyze images of the resulting tests captured by a standard desktop scanner to 1) slightly improve diagnosis of IDA—sensitivity of 90% (83–96%) and a specificity of 77% (64–87%), and 2) predict several important red blood cell parameters, such as mean corpuscular hemoglobin concentration. These results suggest that the use of AMPS combined with machine learning provides an approach to developing point-of-care hematology.

Received 10th July 2016,
Accepted 30th August 2016

DOI: 10.1039/c6lc00875e

www.rsc.org/loc

Introduction

Over one billion people are estimated to suffer from iron deficiency anemia (IDA). As a result of depleted iron stores in the body, adults may experience chronic fatigue, among other symptoms.[1] IDA during pregnancy increases the risk of preterm birth and low birth weight;[2] infants with untreated IDA can have permanent cognitive impairments and delayed physical development.[3] Iron supplements provide a simple intervention to treat IDA, but the use of iron supplements when IDA is not present can result in iron overload.[4] The correct diagnosis of IDA is important to provide patients with effective care. While current clinical capabilities can effectively diagnose IDA in the developed world, many countries lack the expensive instrumentation necessary to detect IDA, especially at the point-of-care.[5]

Red blood indices—measurements of the properties and numbers of red blood cells—are commonly used for the diagnosis of IDA, because they (in contrast to serum iron or ferritin) respond quickly to changes in the iron level in the body, and require a less painful and less invasive procedure for the patient than the gold standard measurement (iron in bone marrow).[6] Red blood cell indices measured by a complete blood count require a hematology analyzer (a flow cytometer, typically with impedance, photometry, and chemical staining capabilities). A hematology analyzer, however, is expensive ($20 000–$50 000) and requires highly trained personnel and significant technical maintenance. An inexpensive, rapid, and simple method that approaches the specificity and sensitivity provided by a hematology analyzer could find widespread clinical use.

An inexpensive tool for the diagnosis of IDA—especially one appropriate for point-of-care (POC)—is mainly needed in resource-limited countries where the rate of IDA is often high

[a] *Department of Chemistry and Chemical Biology, USA*
[b] *School of Engineering and Applied Sciences, USA*
[c] *Department of Neurobiology, Harvard Medical School, USA*
[d] *Department of Laboratory Medicine, Boston Children's Hospital and Department of Pathology, Harvard Medical School, USA.*
E-mail: gwhitesides@gmwgroup.harvard.edu
[e] *Wyss Institute for Biologically Inspired Engineering, USA*

† Electronic supplementary information (ESI) available. See DOI: 10.1039/c6lc00875e

—affecting nearly 20% of the population—and where hematology analyzers are only available in major hospitals.[7]

Identifying microcytic, hypochromic anemia is a potential method to screen for IDA

"Anemia" is defined as a condition in which the patient has a low hemoglobin concentration (HGB) in the blood.[8] Various methods have been developed to diagnose anemia in low-resource settings, either by measuring the number of red blood cells (RBCs) per unit volume through spun hematocrit (HCT), or by measuring HGB directly. Anemia, both chronic and acute, can, however, have many causes, and a diagnosis limited to "anemia" with no further detailed cellular and/or molecular description does not necessarily provide enough information for the effective treatment of a patient.

Anemia associated with microcytic (*i.e.*, smaller cells than normal) and hypochromic (*i.e.*, lower concentration of hemoglobin per cell than normal) cells, on the other hand, is mostly a result of IDA or thalassemia trait (α or β-thalassemias).[9,10] IDA affects >10 times more people globally than does β-thalassemia trait.[7,11,12] Due to the dominance of IDA among other conditions causing microcytic, hypochromic (micro/hypo) red blood cells, several studies have shown good diagnostic accuracy for IDA by measuring the number of hypochromic red blood cells.[13–15] Micro/hypo anemias are also associated with a reduction in the mass density of red blood cells.[16–18]

A tool to distinguish micro/hypo anemia, and thus IDA, quickly from normal blood and other forms of anemia would improve the effectiveness of healthcare, and promote a better use of resources at the level of primary healthcare, in resource-limited countries.

Aqueous multiphase systems (AMPS) can identify the presence of low density red blood cells present in micro/hypo anemia

Aqueous multiphase systems (AMPS) are aqueous solutions of polymers and salts that spontaneously phase segregate and form discrete, immiscible layers.[19–25] Between each phase is an interface with a molecularly sharp step in density; these steps can be used to separate subpopulations of cells by density. The phases of an AMPS can be tuned to have very small differences in density ($\Delta\rho < 0.001$ g cm^{-3}), can be made biocompatible, are thermodynamically stable, and reform if shaken. These properties make AMPS useful for separating cells; the stability of these systems removes the need for gentle handling that traditional gradients in density require, and makes AMPS particularly well suited for applications in point-of-care diagnostics. We previously used AMPS as a tool to enrich reticulocytes from whole blood,[26] and to detect sickle cell disease.[27,28]

Here, we demonstrate the use of AMPS to diagnose IDA, by exploiting the fact that RBCs in patients with micro/hypo anemia have lower density than those of healthy patients. Using only a drop of blood (a volume easily obtainable from a finger prick), we can detect, by eye, low density RBCs and diagnose IDA in under three minutes; this method had a true positive rate (sensitivity) of 84%, with a 95% confidence interval (CI) of 72–93%, and a true negative rate (specificity) of 78% (CI = 68–86%).[29]

We can slightly improve the diagnostic accuracy of our system by imaging each AMPS test with a digital scanner and analyzing the distribution of red color—corresponding to the RBCs—found in the tube. Using standard machine learning protocols,[30–32] we are able to diagnose IDA with a sensitivity of 90% (83–96%) and a specificity of 77% (64–87%), and were able to detect hypochromic RBCs above a threshold of 3.9% with a sensitivity of 96% (CI = 88–99%) and a specificity of 92% (CI = 84–97%). These results suggest that a simple optical reader paired with appropriate algorithms could provide rapid, reader-insensitive diagnosis.

Interestingly, using machine learning, we can also predict many of the important values measured during a complete blood count (namely, values pertaining to red blood cells or "red blood cell indices"). Red blood cell indices are used to diagnose many diseases and, therefore, predicting their values quickly and simply may be clinically useful.

Experimental design

The sedimentation rate of red blood cells is related to important red-cell indices

The sedimentation rate of red blood cells through a fluid is a function of several physical characteristics of the cells: mass, volume, size, shape, deformability, and density (mass per unit volume). These characteristics are related, directly or indirectly, to a number of red blood cell indices, including, mean corpuscular volume (MCV, fL) or the average size of a red blood cell, mean corpuscular hemoglobin (MCH, pg per cell) or the average amount of hemoglobin per cell, mean corpuscular hemoglobin concentration (MCHC, g dL^{-1}) or the average amount of hemoglobin per volume of blood, red blood cell distribution width (RDW, %) or the distribution in volume of the RBCs. These characteristics, in addition to the hematocrit (HCT)—the ratio of the volume of the RBCs to the total volume of blood—can be used to derive the total number of RBCs (#RBCs) and the total hemoglobin concentration in the blood (HGB, g dL^{-1}).

Many hematology analyzers use these indices to categorize red blood cells. The percentage of red blood cells that are microcytic (% micro) is defined as the fraction of cells below a specific MCV. The percentage of red blood cells that are hypochromic (% hypo) is defined as the fraction of cells below a specific MCHC.

The hematology analyzer used in this study (ADVIA 2120, Siemens) defines % micro as the percentage of RBCs of MCV < 60 fL and % hypo as the percentage of RBCs with MCHC < 28 g dL^{-1}. IDA corresponds to a decrease in MCV, MCH, MCHC, and HGB, and an increase in RDW, % hypo, and % micro.[33] Several other hemoglobinopathies have been shown to affect the density of RBCs and could affect the

performance of a density-based test. Sickle cell disease,[34] and spherocytosis[35] are known to increase the density of some or all of the population of RBCs, while β-thalassemia,[33] α-thalassemia,[36] and malaria[37] decrease RBC density.

Classifying blood samples using hematological indices

Here, we discuss several conditions with overlapping population. Using hematological parameters (*i.e.*, red blood cell indices), we define four different states: 1) hypochromia—the condition of having hypochromic RBCs—as % hypo ≥ 3.9%, 2) micro/hypo anemia—the condition of having hypochromic RBCs and low HGB—as % hypo ≥ 3.9% and when HGB < 12.0 g dL^{-1} for females over 15 years, <13.0 g dL^{-1} for males over 15 years, <11.0 g dL^{-1} for children under 5 years, and <11.5 g dL^{-1} for children 5 to 15 years,[8] 3) IDA as micro/hypo anemia when % micro/% hypo ≤ 1.5, and 4) β-thalassemia trait for % micro/% hypo > 1.5.[5,13,38] Fig. S1† is a flow chart illustrating the classification.

Designing AMPS to identify micro/hypo RBCs

AMPS are aqueous buffered mixtures of biocompatible polymers that spontaneously separate into thermodynamically stable layers (*i.e.*, phases) possessing distinct densities. We have previously demonstrated over 300 AMPS ranging from two to six phases.[19] An AMPS with n total phases will contain $n + 1$ interfaces (*e.g.* in a two-phase system: air/top phase, top phase/bottom phase, and bottom phase/container). In order to detect the presence of microcytic and hypochromic red blood cells, a properly designed AMPS should: i) have a top layer with density greater than that of plasma and its components (≥1.025 g cm^{-3}) in order to minimize dilution of the AMPS,[39] ii) have a bottom layer less dense than the average red blood cell density (which are represented by a Gaussian distribution where mature erythrocytes have a density of 1.095 g cm^{-3} and immature erythrocytes (*i.e.*, reticulocytes) of 1.086 g cm^{-3}) such that normal blood will pack at the bottom of the tube,[40–42] iii) maintain biocompatibility by tuning the pH (7.4) and osmolality (290 mOsm kg^{-1}) to match blood,[43] and iv) undergo phase separation in a short amount of time (≤5 minutes) under centrifugation (13 700 g, the typical speed of the StatSpin CritSpin centrifuge used in this study).

We designed a three-phase AMPS (IDA-AMPS) to capture microcytic and hypochromic RBCs at two liquid/liquid interfaces, and to provide information about the density distribution of the RBCs of a patient. IDA-AMPS contained 10.2% (w/v) poly(vinyl alcohol) (78% hydrolyzed, MW ~ 6 kD—poly(vinyl alcohol) is synthesized by hydrolyzing poly(vinyl acetate) to a certain degree, in this case, 78%), 5.6% (w/v) dextran (MW ~ 500 kD), and 7.4% (w/v) Ficoll (MW ~ 400 kD). The density of the phases were ρ_{top} = 1.0505 g cm^{-3}, ρ_{mid} = 1.0810 g cm^{-3}, ρ_{bot} = 1.0817 g cm^{-3} as measured by a U-tube oscillating densitometer (DMA 35, Anton-Paar).

An AMPS diagnostic can be easy to use, rapid, and fieldable

We previously demonstrated the use of a point-of-care assay for sickle cell disease using AMPS.[27,28] A similar strategy is employed here. Briefly, a plastic microhematocrit tube is preloaded with 15 μL of AMPS solution that has been sealed at the bottom with a proprietary white sealant (Critoseal, Leica), and centrifuged for 2 minutes at 13 700 g in a hematocrit centrifuge (CritSpin, Iris Sample Processing) in order to separate the phases.

A drop (5 μL) of blood is loaded at the top of the tube through capillary action enabled by a small hole in the side of the tube;[27] the hole allows the blood to enter the tube up to, but not beyond the hole (by capillary wicking). We previously demonstrated that blood can be loaded using this design with a coefficient of variance (CV) in the volume loaded <4%.[28] An elastomeric silicone sleeve is then slid over the hole to prevent the blood from leaking during centrifugation. Up to 12 tubes can then be loaded at the same time into the hematocrit centrifuge we used and spun for the desired time. In the current study we used a centrifuge that cost ~$1600 (CritSpin, Iris Sample Processing), but our lab has recently transitioned to using a more portable centrifuge manufactured by HWLab (Zhejiane Huawei Scientific Instrument Co. LTD, www.hwlab.cn) that provides similar performance and costs $155 ($60 each for orders >400 units). The cost of the materials and reagents necessary to fabricate a test at the laboratory scale is ~$0.20.[27] The total time needed to perform this assay is less than ten minutes (although it can be done in as little as three minutes, see Results for more details). The power requirement for a small centrifuge, while not ideal, can be met using a battery. A lead-acid 12 V car battery is perhaps the best choice because it is widely available, has a long life cycle, is relatively low cost, and can be charged by nearly every car and truck in the world as well as by solar panels. In situations where battery power is not feasible, human-powered centrifuges could provide the required centrifugal force; our group and others have developed centrifuges using egg beaters, salad spinners, and bicycles, among other methods.[44,45] All of the components for the IDA-AMPS diagnostic, including a car battery to power the centrifuge, can fit into a backpack.[28]

Results and discussion

Visual analysis of IDA-AMPS tests after centrifugation provides a simple diagnostic test for micro/hypo anemia

The diagnostic readout of an IDA-AMPS test is designed for the naked eye to visualize the presence or absence of red color above the packed hematocrit at the bottom of the tube. IDA-AMPS provides three bins of density in which red blood cells can collect: 1) the top/middle (T/M) interface (RBCs ≤ 1.081 g cm^{-3}), 2) the middle/bottom (M/B) interface (RBCs > 1.081 g cm^{-3} and ≤1.0817 g cm^{-3}), and 3) the bottom/seal (B/S) interface (RBCs ≥ 1.0817 g cm^{-3}) (Fig. 1). White blood cells (leukocytes) collect at the T/M interface. In some cases white blood cells can agglomerate with RBCs, resulting in a slight red color at the T/M interface, even in a normal sample.

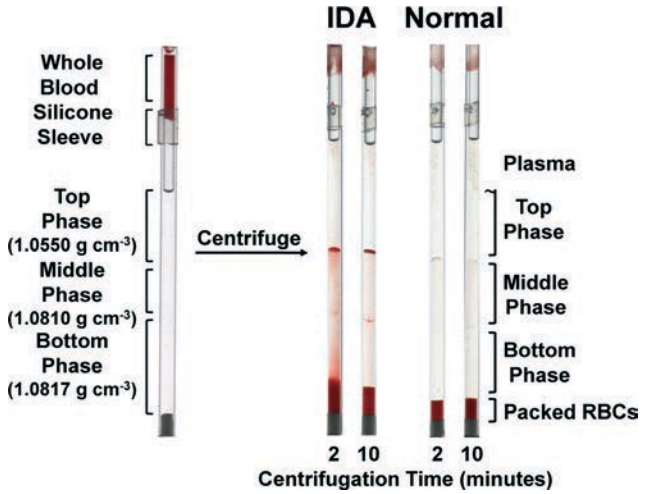

Fig. 1 Design of IDA-AMPS rapid test loaded with blood before and after centrifugation for a representative IDA and Normal sample. Blood is loaded into the top of the tube, from a finger prick, using capillary action provided by a hole in the side of the tube. A silicone sleeve is used to cover the hole to prevent leakage during centrifugation. Normal blood packs at the bottom of the tube, while less dense RBCs can be seen packing at the interfaces between the phases and inside of the phase of the AMPS. Normal and IDA blood can be differentiated, by eye, after only 2 minutes of centrifugation.

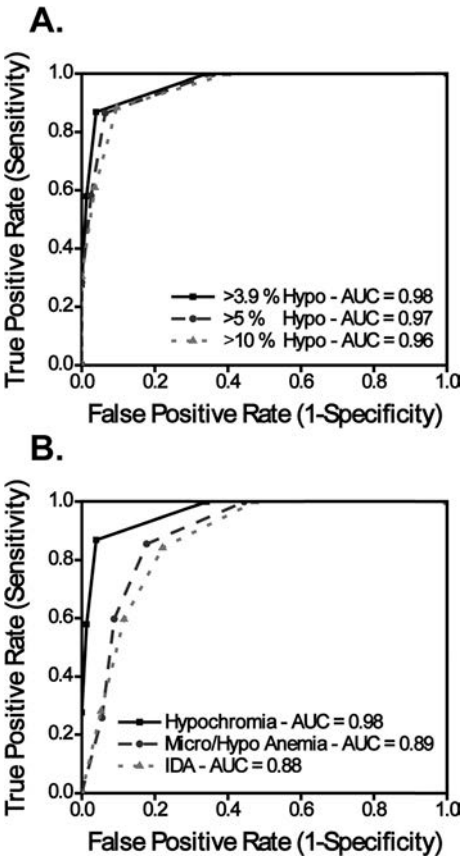

Fig. 2 Receiver operating characteristic (ROC) curves for (A) hypochromia having different threshold values for the percentage of hypochromic red blood cells (% hypo) and (B) diagnosis of hypochromia (% hypo > 3.9%), micro/hypo anemia, and IDA as determined by visual evaluation of the IDA-AMPS test. Each point of the curve represents the sensitivity and specificity of the test for a given redness threshold (1–5) determined by the reader.

Discarded blood samples were obtained from Children's Hospital Boston (n = 152, see Table S2† for a summary of the populations of interest) along with complete blood counts from a hematology analyzer (ADVIA 2120, Siemens). For the purpose of understanding the optimum timing for a test, the assay was performed by stopping centrifugation every two minutes and imaging the tubes using a flatbed scanner (Epson Perfection V330 Photo). After ten minute of centrifugation at 13 700 g, nearly all of the RBCs reached their equilibrium positions; at lower centrifugation times red color was found throughout the phases of the AMPS in samples having micro/hypo RBCs. The time-dependence of the distributions at short centrifugation times provides additional information regarding the size and density distribution of red blood cells. For this reason—and because a rapid test is desirable—we chose results from t = 2 minutes and evaluated the ability of blinded readers to diagnose hypochromia, micro/hypo anemia, and IDA.

Three readers were trained using a guide comprised of images of tests (Fig. S15†) to classify the amount of red color above the packed hematocrit (*i.e.*, the redness threshold) as 1) none or nearly none, 2) some, 3) moderate, 4) strong, and 5) very strong. In some of the cases, red cells were more prevalent at the interfaces, while in others, the red color was highly visible in the phases of the AMPS. The guide was available to readers during each reading for reference. An average score was determined based on concordance between at least two of the readers.

Receiver operating characteristic (ROC) curves were generated (Fig. 2) by varying the redness threshold (1–5) for the diagnosis of hypochromia, micro/hypo anemia, and IDA. A ROC curve is generated by calculating and plotting the true positive rate (sensitivity) *versus* the false positive rate (1 – specificity) at varying threshold values—in this case the redness threshold. The area under the curve (AUC) is highest for hypochromia (0.98, CI = 0.96–1.00); the test is excellent at detecting the presence of hypochromic RBCs. Perfect diagnostic accuracy (*i.e.*, no false positives or false negatives) would result in an AUC = 1.00. The ability to predict micro/hypo anemia and IDA for the IDA-AMPS test is lower, with an AUC of 0.89 (CI = 0.83–0.94) and 0.88 (CI = 0.81–0.94). For IDA, this corresponds to a sensitivity of 84% (CI = 72–93%) and a specificity of 78% (CI = 68–86%) at a maximum efficiency cutoff threshold of redness >2 (some red above the packed hematocrit).

As a diagnostic for IDA, the performance of IDA-AMPS (AUC = 0.89) exceeds that of using only hemoglobin concentration (AUC = 0.73)[46] (often the only metric available in low-resource settings). The AUC, sensitivity, and specificity of IDA-AMPS is also comparable to that of a test for IDA using the reticulocyte hemoglobin concentration (CHr)—a red blood cell parameter measured by a hematology analyzer

(AUC of 0.91, sensitivity of 93.2% and a specificity of 83.2%).[47] Although not perfect, this performance for CHr has been high enough to gain popularity in clinical use.[48] The similar AUC of our test for diagnosing IDA (0.89 *vs.* 0.913) suggests that it could be clinically useful as well, especially in LMICs where a hematology analyzer is often unavailable.

We analyzed the concordance between blinded readers and found excellent *intra*-reader agreement for duplicates of the sample blood sample. On average the three readers showed a Lin's concordance correlation coefficient, ρ_c of 0.99 (a ρ_c of 1.00 is perfect concordance).[49] *Inter*-reader agreement was slightly lower; we found a ρ_c of 0.91 between the three readers (Table S3†). These results suggest that 1) the IDA-AMPS tests are highly reproducible for the same samples, and 2) the lower *inter*-reader agreement may be improved with additional training for the readers.

Digital analysis of IDA-AMPS improves diagnostic performance

We sought to improve our ability to diagnose IDA, or, at the very least, provide reader-insensitive and automated method to make this diagnosis, by analyzing the images obtained using a flatbed scanner. Digital analysis of the AMPS tests was performed using the following steps (Fig. 3): i) a flatbed scanner in transmission mode imaged up to 12 tests simultaneously (Epson Perfection V330 Photo), ii) using a custom program written in Python (iPython Notebook) individual capillary tubes were detected and cropped, and the tube image was converted to hue-saturation-value (HSV) colorspace, iii) the HSV value of each pixel was converted to its corresponding S/V value, and iv) a one dimensional plot of "red intensity" *versus* distance above the (cropped) seal was compiled by summing the S/V values for each row of pixels and saved for later analysis. Further details can be found in the ESI.†

Fig. 4 shows, for a representative normal (A) and IDA (B) sample, i) a scanned test image, ii) its corresponding red intensity image where each pixel was converted to S/V, iii) 1-dimentional red intensity trace, and iv) the first derivative of the 1-dimentional red intensity trace. Digital analysis of images of the IDA-AMPS tests enables the direct comparison of a large number of samples. In Fig. 5, the average red intensity for all normal and micro/hypo samples is plotted as a function of distance from the sealed (bottom) end of the tube for different centrifugation times; the shaded region represents the 99% confidence intervals. The red intensity is highest at distance = 0 cm where the hematocrit packs at the bottom of the tube (the white plastic seal is excluded during analysis and the loading end of the tube is excluded from Fig. 5 for clarity). After 2 minutes of centrifugation, the red intensity difference between the normal and micro/hypo anemic samples in the majority of the tube is high; most of the red color is spread throughout the phases. As the centrifugation time increases, the signal decreases in the phases and increases at the interfaces as red blood cells reach their equilibrium position based on their density.

Machine learning can diagnose IDA as an alternative to blinded readers

Machine learning is a powerful approach for finding an efficient way to make predictions or decisions from data.[31,32] The general problem of predicting classes, or labels, from data is called "classification." Here we apply standard machine learning techniques to the classification problem of distinguishing micro/hypo anemic samples from normal samples using images of the IDA-AMPS test. See the ESI† for more details.

Using the red intensity traces as input data, we trained a machine-learning algorithm (logistic regression) to discriminate micro/hypo anemic from normal samples; each sample was given a score based on its difference from an average normal sample. Using these scores, receiver operating characteristic (ROC) curves were generated for IDA-AMPS for t = 2, 4, 6, 8, and 10 min by changing the decision threshold for micro/hypo anemia using the assigned score. Fig. 6A shows

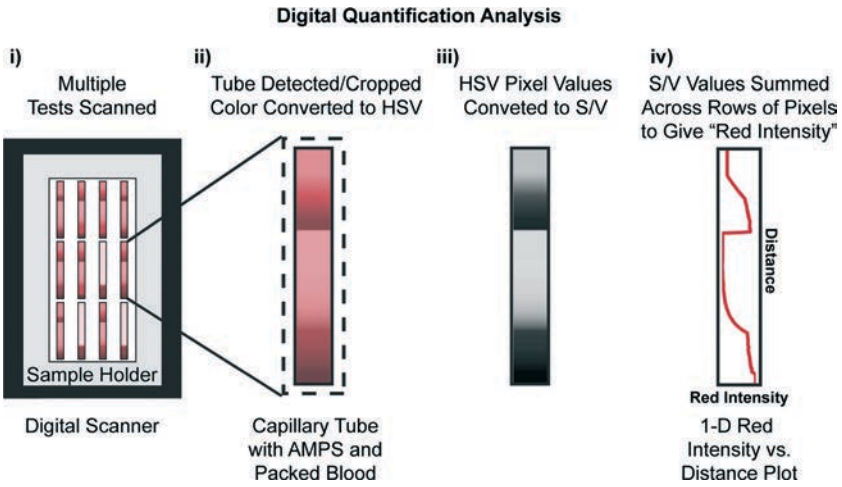

Fig. 3 Schematic of the method used to analyze the quantity and location of red blood cells in an AMPS test using a digital scanner and a custom computer program.

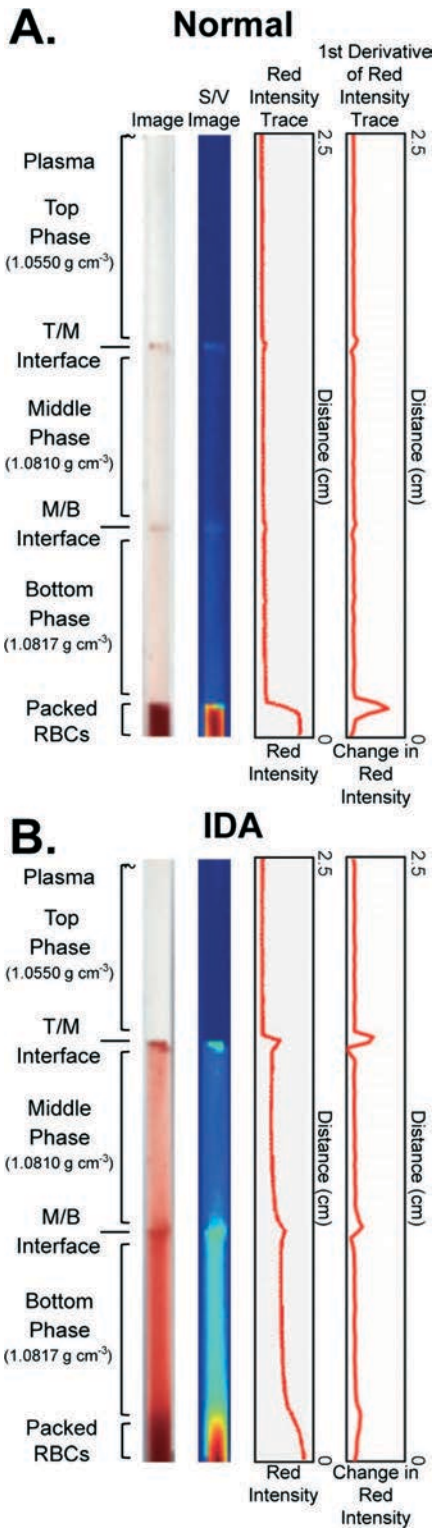

Fig. 4 Examples of IDA-AMPS tests after 2 minutes of centrifugation for a representative normal (A) and IDA (B) sample. Included is an image of the tube and its corresponding image with pixels converted to S/V, 1-D red intensity trace, and the first derivative of the trace. Normal RBCs packs at the bottom of the tube, similarly to a hematocrit, while less dense RBCs can be seen packing at the interfaces between the phases and inside of the phases of the AMPS. White blood cells (leukocytes) pack at the T/M interface and can sometimes agglomerate with RBCs, even in normal blood, causing a slight red color at the T/M interface. For clarity the top (loading port) of the tubes is not shown.

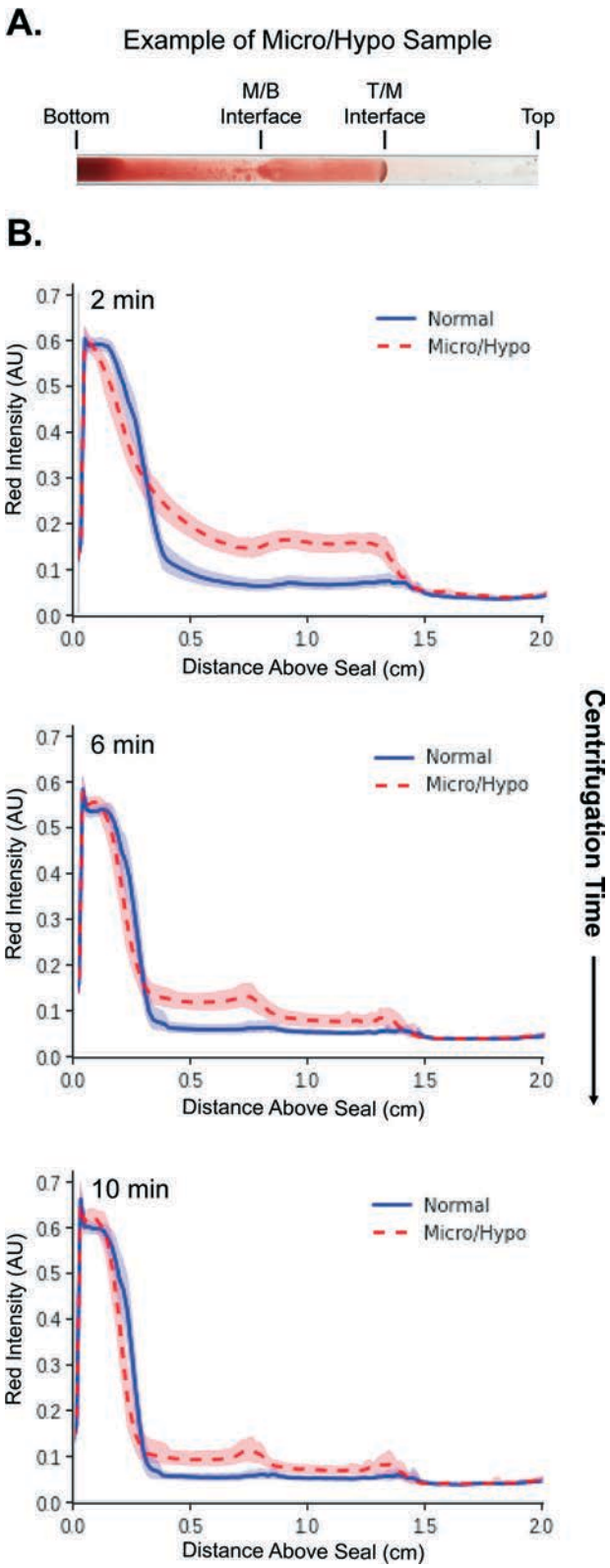

Fig. 5 A) Example of micro/hypo sample (laid on its side) after 2 minutes of centrifugation and B) red intensity *versus* distance plots averaged for 152 samples showing discrimination between normal (solid blue) and micro/hypo anemic (dashed red) samples at 2, 6, and 10 minutes centrifugation.

the area under the curve (AUC) values obtained from these ROC curves. The algorithm randomly samples from the dataset and optimizes the hyperparameters using a validation set of data, and then repeats the process many times. Once the algorithm has been optimized using the training and validation data sets, it analyzes the test data set only one time. For this reason, the results for the AUC calculation are presented without error bars. At short centrifugation times, the test provides excellent discrimination for micro/hypo anemia; the AUC for IDA-AMPS diminishes after 6 minutes of centrifugation. These data suggest that the optimum centrifugation time for the assay is 2 minutes.

Using the machine learning algorithm, we are able to distinguish hypochromia from normal samples with an AUC of 0.98. For micro/hypo anemia we found an AUC of 0.93, and for IDA we found an AUC of 0.90, corresponding to a sensitivity of 90% (CI = 83–96%) and a specificity of 77% (CI = 64–87%) (Fig. 6B). Table 1 provides a comparison of AUC values for visual and digital (machine learning) evaluation of several important subpopulations. These results indicate 3 things: 1) both digital and visual analysis are excellent at detecting the presence of hypochromic RBCs (*i.e.* hypochromia). 2) In all cases, the machine learning results are either slightly better or similar to visual evaluation. Depending on the use case, this suggests that the IDA-AMPS test might be best used alongside a low-cost optical detector (*e.g.*, a desktop scanner) or read by the naked eye, with some trade-off between cost and diagnostic accuracy. 3) Interestingly, our test is able predict hypochromia, micro/hypo anemia, and IDA in women better than men. The AUC for all women in our data set (n = 74) is 0.95 compared to 0.86 for men (n = 78) and, impressively, is a perfect 1.00 for women ≥15 years (n = 47). This difference may be because the normal range of HGB and MCV for women is lower than for men and the current density of the phases of the AMPS used here is closer to the density of RBCs in female blood.[50] An AMPS with a slightly denser bottom phase density might improve the performance in diagnosing the male population (though with a possible tradeoff in performance for women).

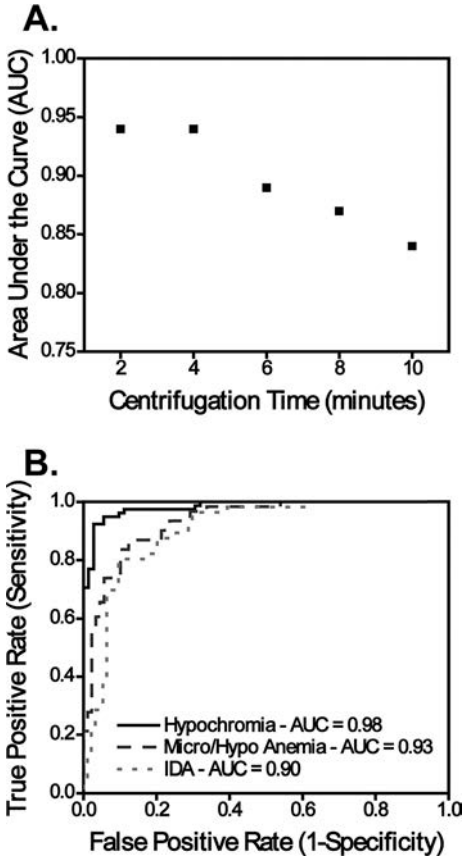

Fig. 6 A. Area under the curve (AUC) values for classifying micro/hypo anemia at 2–10 minutes centrifugation time determined by machine learning (n = 152). Perfect diagnostic accuracy (compared to classification by a hematology analyzer) would result in an AUC = 1.00. For the IDA-AMPS test, the best discrimination between normal and micro/hypo anemic samples is, therefore, at 2 or 4 minutes centrifugation. B. Receiver operating characteristic (ROC) curves for diagnosis of hypochromia (% hypo > 3.9%, solid black line), micro/hypo anemia (dashed red line), and IDA (dotted blue line) as determined by machine learning.

The IDA-AMPS system did not differentiate between IDA and thalassemic traits

One potential confounding factor for a diagnostic that evaluates the presence of low-density RBCs is other hemoglobinopathies. Beta-thalassemia minor (*i.e.* β-thalassemia trait, β-TT) and α-thalassemia trait are benign genetic disorders that can present a confounding diagnosis to IDA because both conditions result in microcytic and hypochromic red blood cells. Identification of thalassemic trait is desired to aid (through genetic counseling) in prevention of β-thalassemia major, HbH disease, and hemoglobin Bart's hydrops fetalis syndrome.[10] Misdiagnosis of β-TT as IDA has been shown to propagate β-thalassemia major, a condition that requires lifelong blood transfusions.[51] Misdiagnosis of IDA in a thalassemic trait patient who is not iron deficient, on the other hand, may result in unnecessary oral iron supplementation therapy and an increased risk of malaria in pregnant women and young children living in endemic areas.[52] Several RBC indices have been shown to provide discrimination between β-TT from IDA.[53] We were not, however, able to obtain enough β-TT samples to determine the discriminative ability of the test reliably. Testing on a larger population that includes patients with β-TT (and other thalassemias) might be needed for our test to be implemented in regions with a high prevalence of β-TT; many Mediterranean countries have a prevalence approaching 10%.[12] Many countries in Sub-Saharan Africa and parts of India, however, have a prevalence of β-TT <3% and some level of uncertainty in differentiating β-TT and IDA might be acceptable.[54]

Machine learning can be used to predict red blood cell indices

In the process of identifying micro/hypo anemia, we noticed that the characteristic curves of red intensity provided an

Table 1 Area under the curve (AUC) and 95% confidence interval (CI) results for diagnosing hypochromia, micro/hypo anemia, and IDA using visual and digital analysis of the IDA-AMPS system after 2 minutes centrifugation

	Visual			Digital		
	Hypochromia	Micro/hypo anemia	IDA	Hypochromia	Micro/hypo anemia	IDA
Population	AUC (CI)	AUC (CI)	AUC (CI)	AUC (CI)	AUC (CI)	AUC (CI)
General (n = 152)	0.98 (0.96–1.00)	0.89 (0.83–0.94)	0.88 (0.81–0.94)	0.98	0.93	0.90
M (n = 78)	0.95 (0.90–1.00)	0.87 (0.79–0.96)	0.80 (0.70–0.91)	0.97	0.91	0.86
F (n = 74)	1.00 (0.99–1.00)	0.91 (0.82–0.99)	0.91 (0.83–0.99)	0.99	0.95	0.95
Age $\geq$ 15 years (n = 47)	0.98 (0.94–1.00)	0.97 (0.91–1.00)	0.97 (0.91–1.00)	1.00	1.00	1.00
Age $\geq$ 5 years, $<$ 15 years (n = 40)	0.95 (0.86–1.00)	0.92 (0.82–1.00)	0.88 (0.76–1.00)	0.95	0.91	0.91
Age $<$ 5 years (n = 65)	0.97 (0.93–1.00)	0.83 (0.72–0.93)	0.82 (0.70–0.93)	0.98	0.86	0.86

information-rich picture of the dynamics of red blood cells moving through AMPS. The way in which an object moves through an AMPS is related to the density, shape, and size of that object. Many of the parameters measured by a hematology analyzer—so called red blood cell indices—should be related to the distribution and movement of red blood cells in an AMPS. Given the ability of our machine learning approach to identify micro/hypo anemia as well as a trained human user, we tested the ability to use the images of blood moving through the IDA-AMPS tests to predict common red blood cell indices. A rapid and inexpensive test that could predict red blood cell indices could have important clinical implications.

Using standard machine learning techniques for this "regression" problem, we were able to predict red blood cell indices from the 1D representation of the output of the IDA-AMPS system (see ESI† for details).[30–32] We guarded against over-fitting using repeated random sub-sampling validation, in which we randomly sampled a training set and a validation set 500 times, and averaged the performance across all validation sets. For each blood parameter we wished to predict, we independently repeated our cross-validated training approach. We included blood parameters we believed would yield good regression performance (those related to red blood cells, % hypo, HGB) and as negative controls, those that the IDA-AMPS system would not be able to detect (those related to colorless cells outside of the density range of our system, WBC, PLT).

True blood parameters, as measured by a hematology analyzer, are compared with predicted parameters determined by machine learning in Fig. 7 and Fig. S2–S14.† Fig. 7B shows a Bland–Altman plot for comparing predicted and true % hypo. % hypo showed the best correlation with a Pearson's r of 0.94 while the other blood cell indices showed a lower correlation (Table 2). As a comparison, other point-of-care tests used to measure HGB (some commercially available) have been found to have r = 0.85–0.96.[55–57] A Pearson's r of 1.00 would represent perfect correlation between the machine learning predictions and the values measured by the hematology analyzer. The ability of a machine learning algorithm to predict any variable in a regression problem is related to the total size of the data set. While the number of patients tested here are substantial for a prototype POC device, the predictive ability of the algorithm could likely be improved by increasing the size of the data set.

One risk of machine learning is over-fitting. To guard against this we evaluated the tests performance for negative

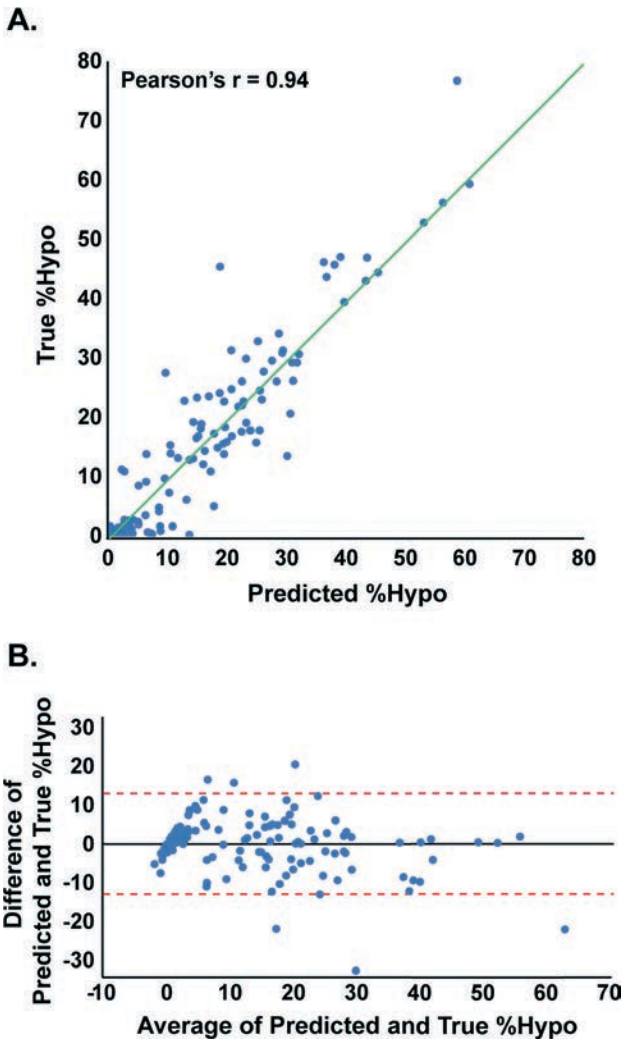

Fig. 7 A. Machine learning prediction results for % hypo (predicted % hypo) compared to a hematology analyzer (true % hypo) and B. Bland–Altman plot showing good agreement between true and predicted % hypo (n = 152). In both cases repeated random sub-sampling validation (n = 500) was used to guard against over-fitting.

Table 2 Pearson product-moment correlation coefficient (Pearson's *r*) for several important blood indices demonstrating the predictive ability of the machine learning algorithm using the IDA-AMPS test. A Pearson's *r* of 1.00 represents perfect positive correlation. As a comparison, other point-of-care tests used to measure HGB (some commercially available) have been found to have *r* = 0.85–0.96 (ref. 55–57)

Blood parameter	Pearson's *r*
% hypo	0.94
MCHC	0.80
CH	0.80
HGB	0.78
HCT	0.76
MCH	0.73
RDW	0.71
HDW	0.68
% micro	0.65
% micro/hypo	0.63
RBC	0.60
% hyper	0.50
MCV	0.49
% macro	0.30

controls that should not correlate to images being evaluated (WBC and PLT) and found, as expected, a very low correlation ($r < 0.2$). Owing to the density of the current test, the algorithm is also unable to predict % macro or % hyper; an AMPS with increased density of the phases might instead be used to identify macrocytosis.

Conclusions

Using aqueous multiphase systems (AMPS), we have created a simple and low-cost method to detect microcytic and hypochromic red blood cells, and hence, IDA. After two minutes in a centrifuge that can be powered by battery, the AMPS test can be evaluated, by eye, and used to diagnose IDA with an AUC of 0.88. Using a desktop scanner to image the tests, we evaluate the images of the IDA-AMPS tests and use standard machine learning protocols to diagnose IDA (AUC = 0.90)—a computer aided diagnosis may be desirable for a fielded device in order to reduce possible user variability. The performance of the IDA-AMPS test is comparable to previous studies[47] using reticulocyte hemoglobin concentration to diagnose IDA (AUC = 0.91) and, therefore, may have a high enough performance to find clinical use.

The WHO estimates that IDA is responsible for ~270 000 deaths and 19.7 million disability-adjusted life years lost annually.[58] Simple interventions, such as oral iron supplements, exist for treating IDA.[59] Supplements, however, should be used only when a diagnosis is available in order to avoid possible side effects. These side effects include iron overload, impaired growth in children, and increased risk of severe illness and death in malaria endemic areas. In developed countries, IDA is easily diagnosed in a central laboratory by a complete blood count and measurement of serum ferritin concentration. In LMICs, however, a lack of instrumentation, trained personnel, and consistent electricity prohibits effective diagnosis. A rapid, low-cost, and simple to use platform to diagnose IDA could find widespread use in LMICs.

To our knowledge, there are currently no direct methods of measuring serum ferritin concentration at the POC. Several methods for measuring hemoglobin—providing a diagnosis for anemia, but not necessarily iron deficiency anemia—are available at the POC. These methods include: 1) the cyanmethemoglobin method using a photoelectric colorimeter,[60] 2) spectrophotometrically using the azidemethoglobin method (*e.g.*, the HemoCue system),[61] 3) colorimetrically (both by eye and a smartphone app) using a redox reaction,[57] 4) paper-based devices,[62] 5) the hematocrit estimate method,[63] and 6) the WHO Hemoglobin Color Scale.[64] Since IDA is a nutritional disorder, molecular diagnostics are not useful for diagnosis, except for a rare hereditary form of IDA called "iron refractory IDA".[65]

The IDA-AMPS test is able to detect microcytic and hypochromic RBCs and diagnose IDA with an AUC comparable to other metrics that have found clinical use, suggesting that it could find widespread use as a screening tool for IDA. In particular, because the equipment needed to run the test is portable,[28] we expect this method to find use in rural clinics where large fractions of the population at risk for IDA, such as children and pregnant women, seek care in LMICs. Ultimately, the performance of this test must be validated in such settings to demonstrate feasibility of using and interpreting the assay.

Using machine learning analysis of digital images, we demonstrate an algorithm that is as good as visual interpretation at identifying IDA; the algorithm determined by the machine learning can be readily implemented into a smartphone application (app). Mobile health—or mHealth, the general term given to portable technologies used to diagnose disease that can transmit data over mobile phone networks—is becoming increasingly widespread in Sub-Saharan Africa.[66,67] By integrating algorithms determined by machine learning into a smartphone app—eliminating the need for visual interpretation and potential bias from users—our test might be used by minimally trained healthcare workers in LMICs. Interestingly, this test may also find use in veterinary medicine. IDA in livestock, especially pigs, is increasingly common due to modern rearing facilities that eliminate the animals' exposure to iron-containing soil; IDA in pigs can cause weight loss, retarded growth, and an increased susceptibility to infection.[68]

A simple method to perform a complete blood count without the need to draw large volumes of blood and send that sample to a central laboratory—so called, point-of-care hematology—has been a major goal of the diagnostic community for several decades. We use machine learning to analyze images of IDA-AMPS tests to predict several red blood cell indices, a first step towards POC hematology. We find, in the best case, a Pearson's *r* of 0.94 for predicting the number of hypochromic RBCs (% hypo). HemoCue, the most widely used portable test used to measure hemoglobin concentration, in comparison, has been shown to correlate nearly perfectly with a hematology analyzer (Pearson's $r = 0.99$) when operated by trained laboratory staff. When the device was used by

clinical staff, however, the correlation was much poorer (Pearson's r = 0.66).[69] The lessons from this study suggest that a POC hematology system needs to be designed to be as simple as possible to operate.

The IDA-AMPS test is a new approach to diagnosing IDA and, using machine learning algorithms, to predict red blood cell indices. Instead of directly measuring a biological marker such as concentration of hemoglobin or serum ferritin, our method relies on observing the way in which red blood cells move through a viscous media (a function of their density as well as size and shape) to make a diagnosis. In the future, this approach may be applied to other diseases or biological applications.

Acknowledgements

The authors thank Rob Miller, Chris Strosahl and Nick Andrews at Drummond Scientific for helpful discussions. This work was supported by an NIH-SBIR grant 1R43HL 123818-01, Bill and Melinda Gates Foundation Award No. 51308, and by CAMTech award #221501 from MGH. A. A. K. acknowledges financial support from the Office of Naval Research through a National Defense Science and Engineering Fellowship. S. Y. R. L. acknowledges financial support from the Harvard College Research Program for undergraduate students.

References

1 S. Killip, J. M. Bennett and M. D. Chambers, *Am. Fam. Physician*, 2007, **75**, 671–678.
2 L. H. Allen, *Am. J. Clin. Nutr.*, 2000, **71**, 1280S–1284S.
3 T. Walter, I. De Andraca, P. Chadud and C. G. Perales, *Pediatrics*, 1989, **84**, 7–17.
4 E. Beutler, A. V. Hoffbrand and J. D. Cook, *Hematology Am. Soc. Hematol. Educ. Program*, 2003, 40–61.
5 Y. Balarajan, U. Ramakrishnan, E. Özaltin, A. H. Shankar and S. V. Subramanian, *Lancet*, 2011, **378**, 2123–2135.
6 J. D. Cook, *Best Pract. Res., Clin. Haematol.*, 2005, **18**, 319–332.
7 N. J. Kassebaum, R. Jasrasaria, M. Naghavi, S. K. Wulf, N. Johns, R. Lozano, M. Regan, D. Weatherall, D. P. Chou, T. P. Eisele, S. R. Flaxman, R. L. Pullan, S. J. Brooker and C. J. L. Murray, *Blood*, 2014, **123**, 615–624.
8 WHO/CDC, *Worldwide prevalence of anaemia 1993-2005*, Geneva, 2008.
9 A. Iolascon, L. De Falco and C. Beaumont, *Haematologica*, 2009, **94**, 395–408.
10 F. B. Piel and D. J. Weatherall, *N. Engl. J. Med.*, 2014, **371**, 1908–1916.
11 R. J. Stoltzfus, *Food Nutr. Bull.*, 2003, **24**, S99–S103.
12 R. Colah, A. Gorakshakar and A. Nadkarni, *Expert Rev. Hematol.*, 2010, **3**, 103–117.
13 S. Kotisaari, J. Romppanen, I. Penttilä and K. Punnonen, *Eur. J. Haematol.*, 2002, **68**, 150–156.
14 E. Urrechaga, L. Borque and J. F. Escanero, *Clin. Chem. Lab. Med.*, 2012, **50**, 685–687.
15 P. Cullen, J. Söffker, M. Höpfl, C. Bremer, R. Schlaghecken, T. Mehrens, G. Assmann and R. M. Schaefer, *Nephrol., Dial., Transplant.*, 1999, **14**, 659–665.
16 D. Danon and Y. Marikovsky, *J. Lab. Clin. Med.*, 1964, **64**, 668–674.
17 B. N. Erickson, H. H. Williams, F. C. Hummel, P. Lee and I. G. Macy, *J. Biol. Chem.*, 1937, **3**, 569–598.
18 G. d'Onofrio, R. Chirillo, G. Zini, G. Caenaro, M. Tommasi and G. Micciulli, *Blood*, 1995, **85**, 818–823.
19 C. R. Mace, O. Akbulut, A. A. Kumar, N. D. Shapiro, R. Derda, M. R. Patton and G. M. Whitesides, *J. Am. Chem. Soc.*, 2012, **134**, 9094–9097.
20 P.-A. Albertsson, *Biochim. Biophys. Acta*, 1958, **27**, 378–395.
21 D. Fisher, *Biochem. J.*, 1981, **196**, 1–10.
22 D. T. Kamei, C. Liu, C. Haase-Pettingell, J. A. King, D. I. C. Wang and D. Blankschtein, *Biotechnol. Bioeng.*, 2002, **78**, 190–202.
23 J. P. Frampton, D. Lai, H. Sriram and S. Takayama, *Biomed. Microdevices*, 2011, **13**, 1043–1051.
24 R. Hatti-Kaul, *Mol. Biotechnol.*, 2001, **19**, 269–277.
25 P. Lutwyche, R. Norris-Jones and D. E. Brooks, *Appl. Environ. Microbiol.*, 1995, **61**, 3251–3255.
26 A. A. Kumar, C. Lim, Y. Moreno, C. R. Mace, A. Syed, D. Van Tyne, D. F. Wirth, M. T. Duraisingh and G. M. Whitesides, *Am. J. Hematol.*, 2014, **90**, 31–36.
27 A. A. Kumar, M. R. Patton, J. W. Hennek, S. Y. R. Lee, G. D'Alesio-Spina, X. Yang, J. Kanter, S. S. Shevkoplyas, C. Brugnara and G. M. Whitesides, *Proc. Natl. Acad. Sci. U. S. A.*, 2014, **111**, 14864–14869.
28 A. A. Kumar, C. Chunda-Liyoka, J. W. Hennek, H. Mantina, S. Y. R. Lee, M. R. Patton, P. Sambo, S. Sinyangwe, C. Kankasa, C. Chintu, C. Brugnara, T. P. Stossel and G. M. Whitesides, *PLoS One*, 2014, **9**, e114540.
29 C. I. Bliss, *Statistics in biology. Statistical methods for research in the natural sciences*, McGraw-Hill Book Company, 1967.
30 H. Drucker, C. J. C. Burges, L. Kaufman, A. J. Smola and V. N. Vapnik, Support Vector Regression Machines, in *Advances in Neural Information Processing Systems 9: NIPS 1996*, MIT Press, 1997.
31 K. P. Murphy, *Machine learning: a probabilistic perspective*, MIT press, 2012.
32 C. M. Bishop, *Pattern recognition and machine learning*, Springer, 2006.
33 G. d'Onofrio, G. Zini, B. M. Ricerca, S. Mancini and G. Mango, *Arch. Pathol. Lab. Med.*, 1992, **116**, 84–89.
34 D. K. Kaul, M. E. Fabry, P. Windisch, S. Baez and R. L. Nagel, *J. Clin. Invest.*, 1983, **72**, 22–31.
35 M.-C. Giarratana, L. Kobari, H. Lapillonne, D. Chalmers, L. Kiger, T. Cynober, M. C. Marden, H. Wajcman and L. Douay, *Nat. Biotechnol.*, 2005, **23**, 69–74.
36 C. T. Noguchi, G. J. Dover, G. P. Rodgers, G. R. Serjeant, S. E. Antonarakis, N. P. Anagnou, D. R. Higgs, D. J. Weatherall and A. N. Schechter, *J. Clin. Invest.*, 1985, **75**, 1632–1637.
37 D. T. X. Trang, N. T. Huy, T. Kariu, K. Tajima and K. Kamei, *Malar. J.*, 2004, **3**, 7.

38 C. Brugnara and N. Mohandas, *Curr. Opin. Hematol.*, 2013, **20**, 222–230.
39 T. Kenner, *Basic Res. Cardiol.*, 1989, **84**, 111–124.
40 F. Bosch, J. Werre, B. Roerdinkholder-Stoelwinder, T. Huls, F. Willekens and M. Halie, *Blood*, 1992, **79**, 254–260.
41 W. H. Grover, A. K. Bryan, M. Diez-Silva, S. Suresh, J. M. Higgins and S. R. Manalis, *Proc. Natl. Acad. Sci. U. S. A.*, 2011, **108**, 10992–10996.
42 R. C. Leif and J. Vinograd, *Proc. Natl. Acad. Sci. U. S. A.*, 1964, **51**, 520–528.
43 A. Kratz, M. Ferraro, P. M. Sluss and K. B. Lewandrowski, *N. Engl. J. Med.*, 2004, **351**, 1548–1563.
44 J. Brown, L. Theis, L. Kerr, N. Zakhidova, K. O'Connor, M. Uthman, Z. M. Oden and R. Richards-Kortum, *Am. J. Trop. Med. Hyg.*, 2011, **85**, 327–332.
45 A. P. Wong, M. Gupta, S. S. Shevkoplyas and G. M. Whitesides, *Lab Chip*, 2008, **8**, 2032–2037.
46 C. Ullrich, A. Wu, C. Armsby, S. Rieber, S. Wingerter, C. Brugnara, D. Shapiro and H. Bernstein, *JAMA, J. Am. Med. Assoc.*, 2005, **294**, 924–930.
47 C. Brugnara, B. Schiller and J. Moran, *Clin. Lab. Haematol.*, 2006, **28**, 303–308.
48 C. Brugnara, J. Adamson, M. Auerbach, R. Kane, I. Macdougall and A. Mast, *Clin. Chem.*, 2013, **59**, 740–745.
49 L. I. Lin, *Biometrics*, 1989, **45**, 255–268.
50 A. Kratz, M. Ferraro, P. M. Sluss and K. B. Lewandrowski, *New Engl. J. Med.*, 2004, **351**, 1548–1563.
51 M. Usman, M. Moinuddin and S. A. Ahmed, *Korean J. Hematol.*, 2011, **46**, 41–44.
52 N. Spottiswoode, M. Fried, H. Drakesmith and P. E. Duffy, *Adv. Nutr.*, 2012, **3**, 570–578.
53 A. Demir, N. Yarali, T. Fisgin, F. Duru and A. Kara, *Pediatr. Int.*, 2002, **44**, 612–616.
54 D. J. Weatherall and J. B. Clegg, *Bull. W. H. O.*, 2001, **79**, 704–712.
55 J. J. Paddle, *Bull. W. H. O.*, 2002, **80**, 813–816.
56 L. Lamhaut, R. Apriotesei, X. Combes, M. Lejay, P. Carli and B. Vivien, *Anesthesiology*, 2011, **115**, 548–554.
57 E. A. Tyburski, S. E. Gillespie, W. A. Stoy, R. G. Mannino, A. J. Weiss, A. F. Siu, R. H. Bulloch, K. Thota, A. Cardenas, W. Session, H. J. Khoury, S. O'Connor, S. T. Bunting, J. Boudreaux, C. R. Forest, M. Gaddh, T. Leong, L. A. Lyon and W. A. Lam, *J. Clin. Invest.*, 2014, **124**, 4387–4394.
58 C. Mathers, G. Stephen and M. Mascarenhas, *Global Health Risks: Mortality and Burden of Disease Attributable to Selected Major Risks*, World Health Organization, 2009.
59 C. Camaschella, *N. Engl. J. Med.*, 2015, **372**, 1832–1843.
60 W. H. Crosby, J. G. Munn and E. D. Furth, *U. S. Armed Forces Med. J.*, 1964, **5**, 693–697.
61 H. von Schenck, M. Falkensson and B. Lundberg, *Clin. Chem.*, 1986, **32**, 526–529.
62 X. Yang, N. Z. Piety, S. M. Vignes, M. S. Benton, J. Kanter and S. S. Shevkoplyas, *Clin. Chem.*, 2013, **59**, 1506–1513.
63 M. M. Strumia, A. B. Sample and E. D. Hart, *Am. J. Clin. Pathol.*, 1954, **24**, 1016.
64 G. J. Stott and S. M. Lewis, *Bull. W. H. O.*, 1995, **73**, 369–373.
65 L. De Falco, M. Sanchez, L. Silvestri, C. Kannengiesser, M. U. Muckenthaler, A. Iolascon, L. Gouya, C. Camaschella and C. Beaumont, *Haematologica*, 2013, **98**, 845–853.
66 T. J. Betjeman, S. E. Soghoian and M. P. Foran, *Int. J. Telemed. Appl.*, 2013, **2013**, 482324.
67 A. Nemiroski, D. C. Christodouleas, J. W. Hennek, A. A. Kumar, E. J. Maxwell, M. T. Fernández-Abedul and G. M. Whitesides, *Proc. Natl. Acad. Sci. U. S. A.*, 2014, **111**, 11984–11989.
68 J. J. Kaneko, J. W. Harvey and M. L. Bruss, *Clinical Biochemistry of Domestic Animals*, Elsevier, 2008.
69 C. Briggs, S. Kimber and L. Green, *Br. J. Haematol.*, 2012, **158**, 679–690.